Resonant Inerter Based Absorbers for a Selected Global Mode

Krenk, Steen

Published in:
Proceedings of the 6th European Conference on Structural Control

Publication date:
2016

Document Version
Peer reviewed version

EACS 2016 – 6th European Conference on Structural Control Sheffield, England: 11-13 July 2016
Paper No. 194

RESONANT INERTER BASED ABSORBERS FOR A SELECTED GLOBAL MODE

S. Krenk

Department of Mechanical Engineering,
Technical University of Denmark, DK-2800 Lyngby, Denmark

sk@mek.dtu.dk

ABSTRACT. The paper presents calibration and efficiency analyses for two different configurations of a resonant vibration absorber consisting of a spring, a damper and an inerter element. In the two configurations the damper is either in parallel with the spring or with the inerter element. A calibration procedure is described for the idealized single structural mass system, starting from the desired level of dynamic amplification, and leading to explicit formulae for the device parameters. The procedure is then extended to a flexible structure by accounting for flexibility and inertia effects from the non-resonant modes. The calibration procedure is given a unified format for the two absorber types, and the high efficiency – evaluated as the ability to reproduce the selected dynamic amplification level of the resonant mode – is demonstrated.

KEYWORDS: Resonant damping, inerter absorber, absorber calibration, non-resonant modes.

1 INTRODUCTION

Damping of resonant vibrations of structures is one of the classic problems of structural dynamics. A particular class is vibration absorber devices using an induced resonance in the device. The classic case is the tuned mass absorber, in which a mass is suspended by a parallel spring-damper. The classic method of calibration consists in adjusting the device parameters to obtain desirable properties of the dynamic response curve, [1]. It has been demonstrated that these attractive properties can be formulated quite simply in terms of the root locus curve generated by the characteristic equation, [2]. An advantage of this approach is that it is easily extended to other resonant absorbers. Recently, an alternative to the absolute motion of a mass has been introduced in the form of the so-called inerter, imposing a pair of inertial forces via the relative motion of two points of fixture, [3, 4], and applications to damping of vibrations of structures have emerged, [5, 6].

While mechanical as well as electromechanical damping devices are easily incorporated into finite element models to enable analysis of the response of the damped structure, there is a need for a design procedure that, based on the essential properties of structure and absorber device, leads to direct formulae for the optimal device parameters. A direct and simple procedure can be developed from the relations obtained in [2]. As it turns out the level of dynamic amplification, contained in the dynamic amplification factor DAF, directly determines the damping ratio of the device, and it is then a simple matter to determine the necessary stiffness and inertia parameters. This procedure was described in detail for the tuned mass absorber in [7], where it was also extended to include the flexibility associated with the

non-resonant background modes. The deformation represented by these modes leads to an increase in the optimal device parameters. This theory was extended in [8], demonstrating the complete equivalence between the tuned mass absorber and an inerter based device in which the inerter is coupled in series with a parallel spring-damper. At the same time a more general representation of the effect of the non-resonant modes was developed, consisting of an inertia term in addition to the more classic background flexibility term.

The present paper gives a brief presentation of an extension of the results from [7, 8] to different resonant inerter based absorber devices and a more direct derivation of the modification of the device parameters arising from the background flexibility and inertia effects. Additional details and examples can be found in [9].

2 STRUCTURE WITH RESONANT AND BACKGROUND MODES

The structure is described by its stiffness, mass and viscous damping matrices **K**, **M** and **C**, respectively. The motion of the structure is described by the displacement vector **u**, satisfying the equation of motion

$$\mathbf{M}\ddot{\mathbf{u}} + \mathbf{C}\dot{\mathbf{u}} + \mathbf{K}\mathbf{u} + \mathbf{f}_d = \mathbf{f}_e, \tag{1}$$

where $\mathbf{f}_e$ is the external load, and $-\mathbf{f}_d$ is the load exerted on the structure by the device. The calibration of the device depends on the frequency response around a resonance frequency and is carried out via a modal analysis.

The calibration of the device is based on a modal analysis of the undamped structure in which the response and forces are assumed implicitly to contain the time variation factor $\exp(i\omega t)$, whereby

$$[\,\mathbf{K} - \omega^2\mathbf{M}\,]\,\mathbf{u} = \mathbf{f}, \tag{2}$$

The eigenfrequencies ω_j and the corresponding mode shape vectors $\mathbf{u}_j$ are determined from the corresponding homogeneous equation

$$[\,\mathbf{K} - \omega_j^2\mathbf{M}\,]\,\mathbf{u}_j = \mathbf{0}, \quad j = 1, \cdots, n \tag{3}$$

where n is the number of degrees-of-freedom of the structural system. When introducing a representation of the response **u** in terms of the mode shape vectors $\mathbf{u}_j$ the solution to (2) is found in the form

$$\mathbf{u} = \Big[\, \sum_{j=1}^{n} \frac{\omega_j^2}{\omega_j^2 - \omega^2} \frac{\mathbf{u}_j\mathbf{u}_j^T}{\mathbf{u}_j^T\mathbf{K}\mathbf{u}_j} \,\Big]\mathbf{f}. \tag{4}$$

This formula contains n terms and a central part of the calibration procedure is to use a simplified approximate form that permits analytical solution of the corresponding characteristic equation.

The calibration procedure considers a load corresponding to the forces from the device acting on the structure. The device connects two degrees of freedom of the structure and the corresponding displacement and force can therefore be expressed in terms of an integer array of the form $\mathbf{w} = [\,0, 0, -1, \cdots, 1, 0\,]$ by the relations

$$u = \mathbf{w}^T\mathbf{u}, \qquad \mathbf{f} = \mathbf{w}\,f. \tag{5}$$

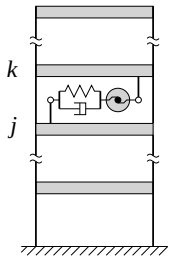

Figure 1: Structure with resonant inerter device.

When using these relations in (4), the local response relation takes the form

$$u = \Big[\sum_{j=1}^{n} \frac{\omega_j^2}{\omega_j^2 - \omega^2} \frac{1}{k_j} \Big] f. \tag{6}$$

where $1/k_j$ is the modal flexibility

$$\frac{1}{k_j} = \frac{(\mathbf{w}^T \mathbf{u}_j)^2}{\mathbf{u}_j^T \mathbf{K} \mathbf{u}_j}. \tag{7}$$

corresponding to the mode shape vector $\mathbf{u}_j/(\mathbf{w}^T\mathbf{u_j})$, normalized to unity at the device.

In the calibration of the device for damping of vibrations around a selected resonant modal frequency ω_r it is desirable to represent the structural response around the resonant frequency as the sum of the resonant response of mode r, plus a suitable simplified representation of the response from the non-resonant modes, $j \neq r$. As demonstrated in [8] a convenient and rather accurate representation of the response around the resonance frequency can be obtained in the form

$$u = \Big[\frac{\omega_r^2}{\omega_r^2 - \omega^2} \frac{1}{k_r} + \frac{1}{k_r'} - \frac{1}{m_r'} \frac{1}{\omega^2} \Big] f. \tag{8}$$

The background stiffness and mass parameters k_r' and m_r' are determined to give the correct full response and the correct frequency derivative at $\omega = \omega_r$.

It was demonstrated that the stiffness and mass parameters k_r' and m_r' can be calculated from a modal analysis based on only the properties of the resonant mode r. First a mass matrix $\mathbf{M}_r$ is introduced, in which the contribution corresponding the the mass of the resonant mode has been removed,

$$\mathbf{M}_r = \mathbf{M} - \frac{(\mathbf{M}\mathbf{u}_r)(\mathbf{u}_r^T \mathbf{M})}{\mathbf{u}_r^T \mathbf{M} \mathbf{u}_r}. \tag{9}$$

This mass matrix is used to define a 'frequency shifted' stiffness matrix

$$\mathbf{K}_r = \mathbf{K} - \omega_r^2 \mathbf{M}_r, \tag{10}$$

in which the resonant mode is left unaffected by the frequency shift. The background flexibility and inertia parameters are then determined explicitly in terms of the system matrices as

$$\frac{1}{k'_r} = \mathbf{w}^T\mathbf{K}_r^{-1}\mathbf{K}\,\mathbf{K}_r^{-1}\mathbf{w} - \frac{1}{k_r}, \qquad \frac{1}{\omega_r^2 m'_r} = \mathbf{w}^T\mathbf{K}_r^{-1}\mathbf{K}\,\mathbf{K}_r^{-1}\mathbf{w} - \mathbf{w}^T\mathbf{K}_r^{-1}\mathbf{w}. \tag{11}$$

It follows from the detailed derivation in [8] that both the background flexibility and inertia coefficients are positive.

3 FREQUENCY RESPONSE OF STRUCTURE WITH DEVICE

The device frequency properties are given by a relation between the displacement u_d over the device and the corresponding force $f_d = -f$,

$$u_d = H'_d(\omega)\, f_d \tag{12}$$

where $H'_d(\omega)$ is the frequency response function of the device. When including this contribution in the response equation (8) the resulting frequency response relation takes the form

$$u = \Big[\underbrace{\frac{\omega_r^2}{\omega_r^2-\omega^2}\frac{1}{k_r} + \frac{1}{k'_r} - \frac{1}{m'_r}\frac{1}{\omega^2}}_{\text{structure with background terms}} + \underbrace{H'_d(\omega)}_{\text{absorber}} \Big] f. \tag{13}$$

In this relation the first term represents the resonant response of mode r, the following two terms represent the approximate response of the non-resonant background modes, and the last term the displacement over the device, characterized by the response function $H'_d(\omega)$ in terms of the stiffness, mass and damping parameters k'_d, m'_d and c'_d.

The calibration procedure developed in the following consists in finding the optimal – or near optimal – location of the complex roots of the response relation (13). This is attained in two steps. The first step identifies the optimal device parameters k_d, m_d and c_d of the corresponding single-mode system

$$u = \Big[\underbrace{\frac{\omega_r^2}{\omega_r^2-\omega^2}\frac{1}{k_r}}_{\text{modal response}} + \underbrace{H_d(\omega)}_{\substack{\text{equivalent}\\ \text{absorber}}} \Big] f, \tag{14}$$

in which the equivalent device response function $H_d(\omega)$ is of the same form as the original device response function $H_d(\omega)$. The device parameters k_d, m_d and c_d that are optimal for (14) solve the single-mode problem, often used in calibration of resonant devices on structures.

The solution for the device parameters k'_d, m'_d and c'_d accounting for the non-resonant background modes are then obtained by considering $H_d(\omega)$ as an equivalent representation of the original system, corresponding to including the background effects into the equivalent device by changing the device parameters. This defines the equivalence relation

$$H_d(\omega) = \frac{1}{k'_r} - \frac{1}{m'_r}\frac{1}{\omega^2} + H'_d(\omega), \tag{15}$$

that in turn enables identification of the background modified parameters k'_d, m'_d and c'_d from the classic single-mode parameters k_d, m_d and c_d.

4 TWO THREE-COMPONENT RESONANT VIBRATION ABSORBERS

Two resonant inerter based vibration absorbers are shown in Fig. 2. They both consist of a spring , a damper and a mass element consisting of an inerter with an equivalent mass, giving the force in terms of the acceleration of the extension of the element. The device stiffness k_d and mass m_d are characterized by the stiffness ratio and the mass ratio,

$$\kappa = \frac{k_d}{k_r}, \qquad \mu = \frac{m_d}{m_r}, \tag{16}$$

where k_r and m_r are the modal stiffness and modal mass of the resonant mode of the structure, defined by (7) and $m_r = k_r/\omega_r^2$, respectively. The device damping is described by the damping ratio

$$\zeta_d = \frac{c_d}{2\sqrt{k_d\, m_d}}. \tag{17}$$

The single-mode design problem consists in finding optimal values of these parameters.

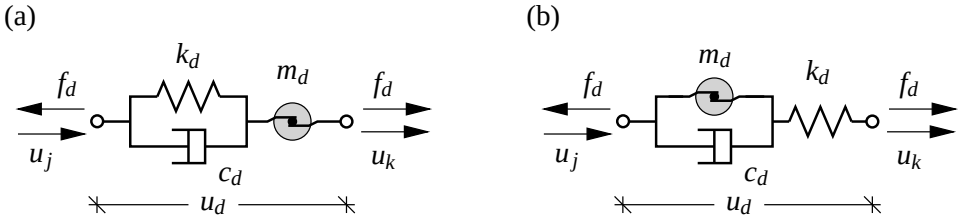

Figure 2: Resonant absorbers. a) parallel spring-damper, b) parallel inerter-damper.

The design is based on a root locus analysis, in which the complex vibration frequencies of the two vibration modes are defined to have identical damping ratio. For the device with parallel spring-damper in Fig. 2a the characteristic equation of the problem follows from the frequency response relation (14) in the form

$$\omega^4 - [(1+\mu)\omega_d^2 + \omega_r^2]\omega^2 + \omega_r^2\omega_d^2 + 2i\zeta_d\omega\omega_d[(1+\mu)\omega^2 - \omega_r^2] = 0. \tag{18}$$

where $\omega_d = \sqrt{k_d/m_d}$ is the device frequency. In the procedure, described in detail in [2, 7], the device frequency ω_d is determined by balancing the coefficients of the linear and cubic terms, using a reference frequency determined by the constant term. This determines the frequency tuning in terms of the mass ratio μ and secures equal damping ratio of the two complex frequencies of the 2-DOF system. At $\zeta_d = 0$ the system is undamped, while increasing damping leads to a bifurcation point in the root-locus diagram. The optimal frequency is a balance between too low damping and the reduction occurring for a double root at the bifurcation point. This determines the device damping ratio ζ_d as function of the mass ratio μ.

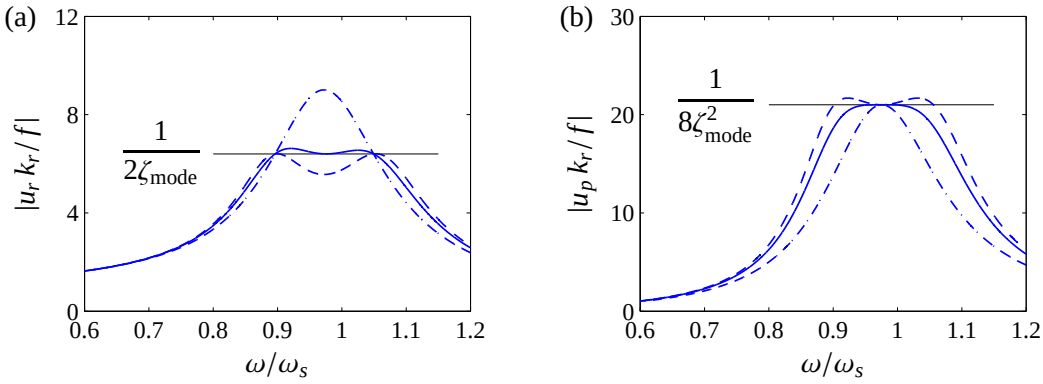

Figure 3: Dynamic amplification of parallel spring-damper for $\mu = 0.05$. a) structure motion u_r and b) relative parallel device element motion u_p. Damping parameter: - - ζ_{classic}, — ζ_{opt}, - · - ζ_{bif}.

A simple design procedure consists in reversing the order of the formulae relative to the derivation. The response of single-mode structure and the corresponding response u_p over the parallel elements in the device are illustrated in Fig. 3 for a mass ratio of $\mu = 0.05$. The design procedure leads to equal damping ζ_{mode} of the two modes, in which the device splits the original undamped single mode. Furthermore, the modal damping ratio is quite accurately represented by $\zeta_{\text{mode}} \simeq \frac{1}{2}\zeta_d$. The amplification levels are indicated in the figure in terms of this modal damping ratio ζ_{mode}. It is observed that the near-level plateau of the dynamic amplification – given by the Dynamic Amplification Factor *DAF* – is described by $DAF \simeq 2\zeta_{\text{mode}}$. In real structures there will be some structural damping, here represented by the damping ratio ζ_{struc}. It has been found in numerical examples that the effective damping ratio describing the amplification similat to those in Fig. 3 can be approximated by the sum of the contribution from the resonant device and the structural damping in the form

$$\zeta_{\text{mode}} \simeq \tfrac{1}{2}\zeta_d + \zeta_{\text{struc}}\,. \tag{19}$$

The design procedure then consists of the following simple steps, shown in the left column of Table 1. First the modal damping ratio ζ_{mode} is determined from the dynamic amplification selected for design. The modal damping ration is then used to calculate the device damping ratio by (19). The device damping ratio determines the mass ratio, and the mass ratio in turn determines the stiffness ratio. In total that gives the physical device parameters given in the last row of the table.

The design of the device with parallel inerter-damper in Fig. 2b is carried out in a similar manner. The characteristic equation following from (14) now takes the form

$$\omega^4 - [\omega_d^2 + (1+\kappa)\omega_r^2]\omega^2 + \omega_r^2\omega_d^2 + 2i\zeta_d\omega\omega_d[\omega^2 - (1+\kappa)\omega_r^2] = 0\,. \tag{20}$$

It is seen that this equation appears rather similar to (18) for the other device, and that the role of the mass ratio μ here is taken over by the stiffness ratio κ. The derivation of the design formulae are the

Table 1: Single-mode design procedure.

	Parallel stiffness-damper	Parallel inerter-damper
Modal damping:	$2\zeta_{\text{mode}} = \dfrac{1}{DAF}$	
Device damping:	$\zeta_d = 2(\zeta_{\text{mode}} - \zeta_{\text{struc}})$	
Mass/stiffness ratio:	$\mu = \dfrac{2\zeta_d^2}{1-2\zeta_d^2}$	$\kappa = \dfrac{2\zeta_d^2}{1-2\zeta_d^2}$
	$\kappa = \dfrac{\mu}{(1+\mu)^2}$	$\mu = \dfrac{\kappa}{(1+\kappa)^2}$
Device parameters:	$m_d = \mu m_r,\ k_d = \kappa k_r,\ c_d = 2\zeta_d\sqrt{m_d k_d}$	

same, and the result – organized in design format – is shown in the right column of Table 1. It is seen that the procedure is quite similar when interchanging the roles of κ and μ. In practical design the values of κ and μ are not too different, but while the parallel spring-damper device tunes the device frequency below the structural frequency, the parallel inerter-damper device tunes the device frequency above the structural frequency.

5 CORRECTION FOR BACKGROUND MODES

In the calculation of the parameters k'_d, m'_d and c'_d the effect of the background flexibility and inertia is described by the non-dimensional coefficients

$$\kappa'_r = \frac{k_r}{k'_r}, \qquad \mu'_r = \frac{m_r}{m'_r}. \tag{21}$$

By the definition of the background parameters in terms of their reciprocals the absence of these effects corresponds to $\kappa'_r = 0$ and $\mu'_r = 0$, respectively.

The device parameters corrected for the effect of the non-resonant background modes are obtained from the equivalence relation (15) by expressing the device response function $H'_d(\omega)$ in terms of the parameters k'_d, m'_d and c'_d and the equivalent device response function $H_d(\omega)$ in terms of the single-mode parameters k_d, m_d and c_d, determined as described in Table 1. Each device has a set of parallel elements as well as a series element. The parameter of the series element can be found directly, whereas the two parameters of the parallel elements require an approximation - essentially consisting in omitting the magnitude of the damping force relative to the direct device force, [8]. The procedure is described in detail in [9]. The results are collected in Table 2. It is seen that all device parameters are increased

Table 2: Correction for background modes.

	Parallel stiffness-damper	Parallel inerter-damper
Background parameters:	$\kappa_r' = \frac{k_r}{k_r'}\,,\ \ \mu_r' = \frac{m_r}{m_r'}$	
Device stiffness:	$k_d' = \frac{k_d}{1-\kappa_r'\,\kappa}$	
Device mass:	$m_d' = \frac{m_d}{1-\mu_r'\,\mu}$	
Device damping:	$c_d' = \frac{c_d}{(1-\kappa_r'\,\kappa)^2}$	$c_d' = \frac{c_d}{(1-\mu_r'\,\mu)^2}$

by the correction for the background modes. The device stiffness and mass are adjusted in the same way for both absorber types via the background parameters κ_r' and μ_r', respectively. The correction of the damper parameter c_r' is larger, and for the parallel stiffness-damper device it is adjusted via the background stiffness coefficient κ_r', while the damping of the parallel inerter-damper device is adjusted via the background inertia coefficient μ_r'.

6 EXAMPLE

The effect of the correction for background modes is illustrated by considering the first three modes of the simple shear frame shown in Fig. 1. Further examples can be found in [8, 9]. The shear building has 10 storeys and the absorber device is connected to the ground and the first floor. The results of the calibration with respect to any one of the first three modes $r = 1, 2, 3$ are given in Table 3 for three different calibration procedures. The first three rows in the table refer to the single-mode calibration described in Table 1. The next block of three rows refers to the so-called quasi-static correction, which is based on a stiffness correction corresponding to setting ω^2 equal to ω_r^2 in the background term in (8). The final block of three rows gives the results for the full quasi-dynamic correction procedure including both a background stiffness and an inertia term. The type of calibration is clear from the parameters κ_r' and μ_r' in the table. In the single-mode procedure they are both zero, in the quasi-static procedure a background stiffness parameter κ_r' is included, and in the quasi-dynamic procedure both background coefficients contribute.

The first block of three rows shows the classic single-mode calibration corresponding to Table 1. The equivalent device damping ratio $\zeta_d = 1/DAF = 0.10$ for all the three modes, and from this follows the mass ratio $m_d'/m_r = 0.0204$, common to all three modes. For an ideal single-mode structure this results in $\zeta_1 = \zeta_2 = \frac{1}{2}\zeta_d = 0.05$. However, as the table shows the effect of the non-resonant background modes leads to considerable unbalance in the modal damping ratios, and thereby to considerable deviation from

Table 3: Absorber in shear frame structure with $DAF = 10$.

r	κ'_r	μ'_r	$\frac{m'_d}{m_r}$	$\frac{\omega'_d}{\omega_r}$	ζ'_d	$\zeta_{1,2}$	
1			0.0204	0.9800	0.1000	0.0587	0.0301
2			0.0204	0.9800	0.1000	0.0575	0.0304
3			0.0204	0.9800	0.1000	0.0546	0.0310
1	4.2795		0.0204	1.0239	0.1140	0.0500	0.0501
2	4.5235		0.0204	1.0266	0.1149	0.0474	0.0519
3	5.0587		0.0204	1.0325	0.1170	0.0416	0.0553
1	4.6877	0.2130	0.0204	1.0261	0.1153	0.0495	0.0516
2	5.7240	1.4584	0.0210	1.0245	0.1177	0.0495	0.0518
3	7.9976	4.1908	0.0223	1.0206	0.1235	0.0494	0.0524

the level plateau marking the dynamic amplification around resonance as illustrated for mode $r = 2$ in Fig. 4, showing the computed response amplification for a mode 2 load distribution.

The results from the quasi-static calibration are shown by the next three-row block. The assumption of this calibration corresponds to the first mode, and this is confirmed by excellent balance of the modal damping ratios $\zeta_1 \simeq \zeta_2 \simeq 0.05$ for this mode. For mode 2 and mode 3 an unbalance appears, but considerably smaller than in the case of single-mode calibration. Finally, the quasi-dynamic calibration

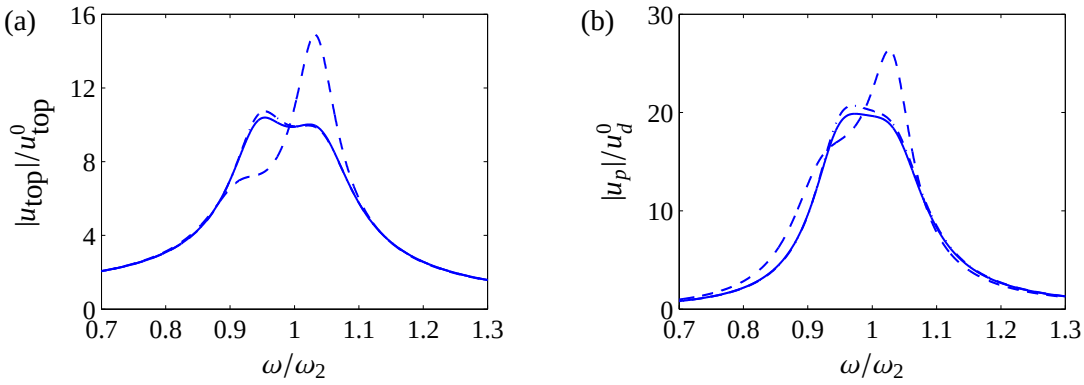

Figure 4: Dynamic amplification with parallel spring-damper for $DAF = 10$. a) structure motion u_r and b) parallel element device motion u_p. Single-mode (- -), quasi-static correction (- · -) and quasi-dynamic correction (—).

procedure with both background coefficients is illustrated in the last three rows. It is seen that the results for the first mode exhibit a slightly larger unbalance than for the quasi-static correction, which is specifically directed towards the first mode. However, the quasi-dynamic correction retains the balance of the modal damping ratios ζ_1 and ζ_2. The good quality of the calibration when including the effect of the background modes is illustrated in Fig. 4.

7 CONCLUSIONS

An overview has been given of a calibration method for a resonant inerter based absorber device targeting a selected mode of a flexible structure, and two inerter based devices are described in detail. The procedure consists of two steps. In the first step the device stiffness, damping and inertia parameters are determined from a selected level of dynamic amplification for the idealized case of a device acting via a single mode representation of the structure. In the second step the preliminary device parameters are modified by simple explicit formulae to account for the non-resonant background modes of the structure, represented by a two-term approximate representation of the additional response from these modes. The whole procedure is explicit in terms of coefficients obtained from the stiffness and mass matrix of the structure plus the frequency and mode-shape of the targeted resonant mode. The calibration procedure appears to be quite accurate – both with respect to reproducing the selected level of dynamic amplification, as well as providing a fairly uniform level of dynamic amplification about the resonance frequency.

REFERENCES

[1] Den Hartog, J.P., *Mechanical Vibrations* (4th edn). McGraw-Hill, NY, 1956. (Reprinted by Dover, NY, 1985)

[2] Krenk, S., Frequency analysis of the tuned mass damper. *Journal of Applied Mechanics*, 2005; **72**:936–942.

[3] Smith, M.C., Synthesis of mechanical networks: The inerter. *IEEE Transactions on Automatic Control*, 2002; **47**:1648–1662.

[4] Chen, M.Z.Q., Papageorgiou, C., Scheibe, F., Wang, F.C. & Smith, M.C., The missing mechanical circuit. *IEEE Circuits and Systems Magazine*, 2009; **9**:10–26.

[5] Lazar, I.F., Neild, S.A. & Wagg D.J., Using an inerter-based device for structural vibration suppression. *Earthquake Engineering and Structural Dynamics*, 2014;**43**:1129–1147.

[6] Marian, L. & Giaralis, A., Optimal design of a novel tuned mass-damper-inerter (TMDI) passive vibration control configuration for stochastically support-excited structural systems. *Probabilistic Engineering Mechanics*, 2014; **38**:156–164.

[7] Krenk, S. & Høgsberg, J., Tuned resonant mass absorber on a flexible structure. *Journal of Sound and Vibration*, 2014; **333**:1577–1595.

[8] Krenk, S. & Høgsberg, J., Tuned resonant mass or inerter-based absorbers: Unified calibration with quasi-dynamic flexibility and inertia correction. *Proceedings of the Royal Society, A*, 2016; **472**:20150718.

[9] Krenk, S., Resonant inerter based vibration absorbers on flexible structures, 2016. (to be published)